

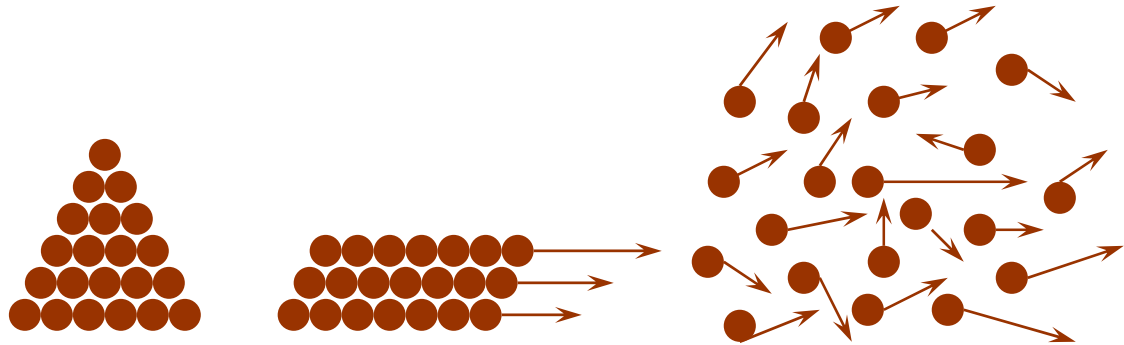
Dense Granular Flow Model Development

Introduction

The following figure shows various granular flow regimes. On the right is the viscous regime, in which the particles exchange momentum through collisions. Such a regime exists in bubbling and circulating fluidized beds. The nature of the granular media in this flow regime is similar to that of ordinary fluids, and the constitutive equations, based on kinetic theory, are well established. In the middle is the plastic regime, in which the particles maintain enduring contact with each other and the momentum transfer between the particles is governed by friction. On the left is the elastic regime, in which the particles are static or non-shearing (no relative movement between particles). In plastic regime flows regions in elastic regime usually appear. Such a flow regime exists in spouted beds, solids flow valves (e.g., L-valve), and standpipes. The behavior of granular medium in elastic-plastic regime is distinctly different from that of ordinary fluids: stresses arise from friction; granular media can resist shear; granular media does not fill available volume; and shear stress varies with pressure.

Because of the distinct behavior of granular media standard constitutive equations cannot describe dense granular flows. For example, if standard equations are used to describe a heap of sand the medium will flow and form a level bed surface. One way to stop the fluid from flowing is to make the viscosity very large. In fact plastic flow theories are defined for static beds and in the limit of shear going to zero a viscosity coefficient in such theories become unbounded. A fix for this problem in computer codes is to limit the value of viscosity to a large value to prevent divide-by-zero errors. This approach will prevent a conical heap of sand from flowing, but does not have any predictive capability. The theory will not be able to predict changes in the slope of the sand pile as the operating condition change. Furthermore the theory will not be able to predict even simple manifestations of elastic-plastic regime such as the pressure distribution in a silo.

<u>Regime</u>	<u>Elastic Regime</u>	<u>Plastic Regime</u>	<u>Viscous Regime</u>
Contact	Static	Enduring contact	Collisional contact
Shearing	None	Slow	Rapid
Stress state	Strain dependent	strain rate independent	Strain rate dependent
Theory	Elasticity	yield surface, flow rule	Kinetic theory



The two approaches we have considered (Elasto-plasticity and Hypoplasticity) for modeling dense granular flow are described in detail below.

Elasto-Plasticity

Yield surface

Flow rule

Decomposition of deformation into plastic and elastic parts

Critical state theory

Problem at zero deformation

Savage

Sundar

An example:

Hypoplasticity

The Cam-clay model based on critical state theory predicts the salient features of clay with 3 easily measured parameters. Attempts to extend the model to describe soil behavior lead to complicated models such as double yield surfaces, bounding surface theory, anisotropic hardening rule, endochronic intrinsic time, etc. Such complicated theories arise because the behavior of sand is more complex than clay: loose sand contracts and dense sand initially contracts and then expands. There are several difficulties with the traditional elastoplasticity models (Wu and Niemunis 1997):

- Decomposition of deformation into elastic and plastic parts.
- Transition between elastic and plastic deformation.
- Switch function to differentiate between loading and unloading.

- Based on the idea of yield surface, the determination of which is rather subjective. Unlike that of metals, the stress-strain curve of granular media does not show clear yielding points.
- Experimental information on critical state is limited. Critical state is attained after continued shear when shear strain increases without change of stress state and the material neither contracts nor dilates. However, the large deformations required to attain critical state makes the system inhomogeneous and measurements difficult (Kolymbas et al. 1995).

Hypoplasticity gets rid of the yield surfaces and the need for switching between the elastic and plastic computations by postulating an equation for the evolution of stress. The theory was pioneered by Kolymbas (1977) at the Institute of Soil and Rock Mechanics of University of Karlsruhe. It is an extension of hypoelasticity and is closely related to endochronic theory. The terminology was first introduced by Dafalias (1986), and the first equations were published by Kolymbas (1977). Kolymbas (1985) later improved them, and Wu (1992) modified the theory so that non-allowable stress states (tensile stress) are not predicted. The theory has been applied to a variety of problems (e.g., Wu and Bauer 1994, Kolymbas et al. 1995, Tejchman and Wu 1996). The term hypoplastic means lacking (plastic) yield surface and plastic potential. Failure surfaces, flow rule and earth pressure coefficient at rest, which have to be prescribed in most elastoplastic models now turn out as natural outcomes of constitutive models.

Wu and Bauer (1994) developed one hypoplastic constitutive theory. Their constitutive equation contained four material constants. Wu and Bauer showed the material constants can be measured by conducting standard tests such as oedometer test, triaxial test, plane strain test and simple shear test. In particular the four constants can be determined from the most widely used triaxial compression test -- a single triaxial compression test under constant confining pressure.

An outline of the hypoplastic theory development is sketched below generally following the contribution of Wu and Bauer (1994). The hypoplastic constitutive model is developed from the starting postulate

$$\overset{o}{S} = H(S, D) \quad (1)$$

where $\overset{o}{S}$ is the Jaumann derivative of the stress S defined as

$$\overset{o}{S} = \frac{\partial S}{\partial t} + v_s \cdot \nabla S + SW - WS \quad (2)$$

The Jaumann derivative enters such a constitutive model as it is an objective time derivative of the stress. Zhang and Rauen Zahn (1997) derived an evolution equation for stress in dense granular flows and showed that the physical origin of such a derivative is the rotation and deformation of the line connecting the centers of contacting particles. D is the deformation rate

$$D = \frac{1}{2} \left(\nabla \mathbf{v}_s + \nabla \mathbf{v}_s^T \right) \quad (3)$$

and W is the vorticity tensor

$$W = \frac{1}{2} \left(\nabla \mathbf{v}_s - \nabla \mathbf{v}_s^T \right) \quad (4)$$

Hypoplastic theory requires that H is non-differentiable in and only in $D = 0$. The non-differentiability of H is the distinguishing feature by which hypoplasticity differs from the hypoelastic theory of Truesdell (?).

In the hypoplastic model the history dependence is reduced to the instantaneous stress state. Non-differentiability of H at $D = 0$ implies that the model is necessarily incrementally non-linear and affords the description of irreversible deformation that occurs in plastic flows. In contrast irreversibility is modeled in elastic-plastic theory by using different functions for loading and unloading.

To determine a functional form of H the theorist starts by applying several restrictions based on physical principles that varies from very general to very specific for soil behavior:

1. Objectivity: The material response described by the constitutive equation should remain invariant under rigid rotations (Truesdell and Toupin). H should satisfy the following condition.

$$H(QSQ^T, \lambda QDQ^T) = QH(S, D)Q^T \quad (5)$$

where Q is an orthogonal tensor.

2. Rate Independence: It is experimentally observed that the stress is independent of shear rate (see for example Schaeffer ?). This translates into a restriction that H is positively homogeneous of the first order in D ; i.e.

$$H(S, \lambda D) = \lambda H(S, D) \quad (6)$$

where λ is an arbitrary positive scalar. This ensures that no material parameter with the dimension of time can enter the constitutive equation.

3. The predicted material behavior must satisfy the following experimental observation of Goldscheider (1982): *A proportional strain (stress) path starting from a nearly stress free and undistorted state yields a proportional stress (strain) path.* This implies that \dot{H} should be homogeneous in S ; i.e.

$$H(\lambda S, D) = \lambda^n H(S, D) \quad (7)$$

where λ is an arbitrary scalar and n is the order of homogeneity. This restriction also implies that experiments conducted at different stress levels can be normalized by $(trD)^n$.

Wu and Bauer (1994) develop a subclass of hypoplastic equation by splitting (without loss of generality) \dot{H} into linear and nonlinear parts.

$$\dot{S}^o = L(S, D) - N(S, D) \quad (8)$$

Now consider the following specific form:

$$\dot{S}^o = L(S) : D - N(S) \|D\| \quad (9)$$

where

$$\|D\| = \sqrt{tr(D^2)} \quad (10)$$

With the non-differentiability introduced in N the difference in loading and unloading come about naturally:

$$\dot{S}^o = \begin{cases} [L - N]D : D > 0 & \text{loading} \\ [L + N]D : D < 0 & \text{unloading} \end{cases} \quad (11)$$

A formula for failure surface may be derived from the hypoplastic equation. A material is said to be at failure if for a given stress S , a strain rate $D \neq 0$ exists such that the stress rate vanishes; i.e.,

$$\overset{o}{S} = H(S, D) = 0 \quad (12)$$

Therefore, the failure surface is $S \in \{S \mid \overset{o}{S} = 0\}$. The critical state is a special case of the above formula when the volumetric strain rate vanishes simultaneously:

$$S \in \{S \mid \overset{o}{S} = 0 \cap \text{tr}D = 0\}. \quad (13)$$

For the subclass of hypoplastic model defined previously, since at failure

$$\overset{o}{S} = L(S) : D - N(S) \|D\| = 0 \quad (14)$$

the strain rate direction is given by

$$\frac{D}{\|D\|} = L^{-1}N \quad (15)$$

Furthermore because

$$\frac{D^T D}{\|D\|^2} = 1 \quad (16)$$

we get the equation for failure surface as

$$f(S) = N^T (L^T)^{-1} L^{-1} N - 1 = 0 \quad (17)$$

Note that failure has two aspects: A kinematic aspect (direction of strain rate) called *flow rule* and given by equation (15); a dynamic aspect (relationship between stress components) called *failure surface* and given by equation (17). Also note that the flow rule is non-associated since in general

$$\frac{f(S)}{\partial S} \neq L^{-1}N \quad (18)$$

Experimental evidence shows that flow rule in granular materials is in general non-associated.

Wu and Bauer (1994) choose the simplest representation of L and N taking them as homogeneous of the first order in σ to get the equation

$$\begin{aligned} \dot{S} = & C_1 \text{tr} S D + C_2 \frac{\text{tr}(SD) S}{\text{tr} S} \\ & + \left(C_3 \frac{S^2}{\text{tr} S} + C_4 \frac{(S^*)^2}{\text{tr} S} \right) \|D\| \end{aligned} \quad (19)$$

where the deviatoric stress is defined as

$$S^* = S - \frac{1}{3}(\text{tr} S) I \quad (20)$$

The constants C_1, C_2, C_3 and C_4 are dimensionless constants that can be determined from standard experiments. Wu and Bauer (1984) lists closed form relations for calculating the constant from a single triaxial test under constant confining pressure.

Some limitations of the model must be noted:

- Stress rate is independent of the way in which the stress state is reached. The memory is contained in the local state of stress. Soils remember the loading history. There is a modified hypoplasticity theory that accounts for memory by including a *back stress* (Kolymbas 1995).
- Reduction in shear strength after failure (strain softening) cannot be modeled.
- In the (simplified) model is homogeneous of the first order in stress tangential stiffness is linearly proportional to stress level and friction angle is independent of the stress level. In reality they both decrease with increasing stress level.

Tejchman and Wu (1996) applied the theory to study shear band formation. When a displacement was applied to a uniform vertical column of sand, the model predicted the formation of a thick pile of sand at the bottom of the column; i.e. the model did not predict any

shear band formation. When an imperfection was introduced into the column of sand – larger void-fraction near the middle of the column – the model predicted shear band formation centered near the imperfection. The shear zone inclination to the horizontal predicted by the theory (54.5°) agreed with experimental data (64°). The thickness of the shear zone predicted by the theory (4.3 mm) did not agree very well with experimental data (8 mm).

Adaption of Hypoplasticity Theory for MFIx

For including hypoplasticity theory in MFIx we adapted the Wu and Bauer (1994) equation (19). As in Tejchman and Wu (1996) the equation was modified to allow the granular medium to contract and dilate by introducing the factor f_c in equation (19):

$$\begin{aligned} \dot{S} = & C_1 \text{tr} S D + C_2 \frac{\text{tr}(SD) S}{\text{tr} S} \\ & + f_c \left(C_3 \frac{S^2}{\text{tr} S} + C_4 \frac{(S^*)^2}{\text{tr} S} \right) \|D\| \end{aligned} \quad (21)$$

where

$$f_c = (1 - a_0) \left(\frac{e - e_{\min}}{e_{\text{crt}} - e_{\min}} \right) + a_0 \quad (22)$$

The void ratio is related to void fraction as

$$e = \frac{\varepsilon}{1 - \varepsilon} \quad (23)$$

The critical void ratio is given by

$$e_{\text{crt}} = e_{\min} + a_1 \exp \left[-a_2 \frac{|\text{tr} S|}{p_a} \right] \quad (24)$$

where p_a is the atmospheric pressure. As an example, a set of material constants for 500 m Karlsruhe medium sand (elastic modulus = 40 Mpa; critical friction angle = 30°) is as follows:

Parameter	Value
C_1	-33.5
C_2	-341.4
C_3	-339.7
C_4	446.5
e_{\min}	0.53
a_0	0.8
a_1	0.31
a_2	0.02

For including the above equation into MFIx, we convert it into a transport equation by multiplying with $\varepsilon_s \rho_s$ and adding the granular continuity equation multiplied by S

$$\frac{\partial \varepsilon_s \rho_s}{\partial t} + \nabla \cdot (\varepsilon_s \rho_s \mathbf{v}_s) = 0 \quad (25)$$

to get

$$\begin{aligned} & \frac{\partial \varepsilon_s \rho_s S}{\partial t} + \nabla \cdot (\varepsilon_s \rho_s \mathbf{v}_s S) + \varepsilon_s \rho_s (SW - WS) = \\ & \varepsilon_s \rho_s \left\{ C_1 \text{tr} S \, D + C_2 \frac{\text{tr}(SD)S}{\text{tr} S} + f_c \left(C_3 \frac{S^2}{\text{tr} S} + C_4 \frac{(S^*)^2}{\text{tr} S} \right) \|D\| \right\} \end{aligned} \quad (26)$$

Following Wu and Bauer (1994) (after fixing some typographical errors in their paper), the above equation is written in component form as follows:

$$\begin{aligned}
& \frac{\partial \varepsilon_s \rho_s S_{11}}{\partial t} + \nabla \cdot (\varepsilon_s \rho_s \mathbf{v}_s S_{11}) \\
& + \varepsilon_s \rho_s (S_{12} W_{21} + S_{13} W_{31} - S_{21} W_{12} - S_{31} W_{13}) = \\
& \frac{\varepsilon_s \rho_s}{tr S} \left\{ \begin{aligned}
& (C_2 S_{11} S_{11} + C_1 tr^2 S) D_{11} \\
& + C_2 S_{11} S_{22} D_{22} \\
& + C_2 S_{11} S_{33} D_{33} \\
& + 2 C_2 S_{11} S_{12} D_{12} \\
& + 2 C_2 S_{11} S_{13} D_{13} \\
& + 2 C_2 S_{11} S_{23} D_{23} \\
& + f_c \|D\| [C_3 (S_{11}^2 + S_{12}^2 + S_{13}^2) + C_4 (S_{11}^{*2} + S_{12}^2 + S_{13}^2)]
\end{aligned} \right\} \\
& (27)
\end{aligned}$$

$$\begin{aligned}
& \frac{\partial \varepsilon_s \rho_s S_{22}}{\partial t} + \nabla \cdot (\varepsilon_s \rho_s \mathbf{v}_s S_{22}) \\
& + \varepsilon_s \rho_s (S_{21} W_{12} + S_{23} W_{32} - S_{12} W_{21} - S_{32} W_{23}) = \\
& \frac{\varepsilon_s \rho_s}{tr S} \left\{ \begin{aligned}
& C_2 S_{11} S_{22} D_{11} \\
& + (C_2 S_{22} S_{22} + C_1 tr^2 S) D_{22} \\
& + C_2 S_{22} S_{33} D_{33} \\
& + 2 C_2 S_{12} S_{22} D_{12} \\
& + 2 C_2 S_{13} S_{22} D_{13} \\
& + 2 C_2 S_{22} S_{23} D_{23} \\
& + f_c \|D\| [C_3 (S_{12}^2 + S_{22}^2 + S_{23}^2) + C_4 (S_{22}^{*2} + S_{12}^2 + S_{23}^2)]
\end{aligned} \right\} \\
& (28)
\end{aligned}$$

$$\begin{aligned}
& \frac{\partial \varepsilon_s \rho_s S_{33}}{\partial t} + \nabla \cdot (\varepsilon_s \rho_s \mathbf{v}_s S_{33}) \\
& + \varepsilon_s \rho_s (S_{31} W_{13} + S_{32} W_{23} - S_{13} W_{31} - S_{23} W_{32}) = \\
& \frac{\varepsilon_s \rho_s}{tr S} \left\{ \begin{aligned}
& C_2 S_{11} S_{33} D_{11} \\
& + C_2 S_{22} S_{33} D_{22} \\
& + (C_2 S_{33} S_{33} + C_1 tr^2 S) D_{33} \\
& + 2 C_2 S_{12} S_{33} D_{12} \\
& + 2 C_2 S_{13} S_{33} D_{13} \\
& + 2 C_2 S_{23} S_{33} D_{23} \\
& + f_c \|D\| \left[C_3 (S_{13}^2 + S_{23}^2 + S_{33}^2) + C_4 (S_{33}^{*2} + S_{13}^2 + S_{23}^2) \right]
\end{aligned} \right\} \\
& (29)
\end{aligned}$$

$$\begin{aligned}
& \frac{\partial \varepsilon_s \rho_s S_{12}}{\partial t} + \nabla \cdot (\varepsilon_s \rho_s \mathbf{v}_s S_{12}) \\
& + \varepsilon_s \rho_s (S_{11} W_{12} + S_{13} W_{32} - S_{22} W_{12} - S_{32} W_{13}) = \\
& \frac{\varepsilon_s \rho_s}{tr S} \left\{ \begin{aligned}
& 2 C_2 S_{11} S_{12} D_{11} \\
& + 2 C_2 S_{22} S_{12} D_{22} \\
& + 2 C_2 S_{33} S_{12} D_{33} \\
& + (2 C_2 S_{12} S_{12} + tr^2 S) D_{12} \\
& + 2 C_2 S_{13} S_{12} D_{13} \\
& + 2 C_2 S_{23} S_{12} D_{23} \\
& + f_c \|D\| \left[C_3 (S_{11} S_{12} + S_{12} S_{22} + S_{13} S_{23}) \right. \\
& \quad \left. + C_4 (S_{11}^* S_{12} + S_{12} S_{22}^* + S_{13} S_{23}) \right]
\end{aligned} \right\} \\
& (30)
\end{aligned}$$

$$\begin{aligned}
& \frac{\partial \varepsilon_s \rho_s S_{13}}{\partial t} + \nabla \cdot (\varepsilon_s \rho_s \mathbf{v}_s S_{13}) \\
& + \varepsilon_s \rho_s (S_{11} W_{13} + S_{12} W_{23} - S_{23} W_{12} - S_{33} W_{13}) = \\
& \frac{\varepsilon_s \rho_s}{tr S} \left\{ \begin{aligned}
& 2 C_2 S_{11} S_{13} D_{11} \\
& + 2 C_2 S_{22} S_{13} D_{22} \\
& + 2 C_2 S_{33} S_{13} D_{33} \\
& + 2 C_2 S_{12} S_{13} D_{12} \\
& + (2 C_2 S_{11} S_{13} + C_1 tr^2 S) D_{13} \\
& + 2 C_2 S_{23} S_{13} D_{23} \\
& + f_c \|D\| \left[C_3 (S_{11} S_{13} + S_{12} S_{23} + S_{13} S_{33}) \right. \\
& \left. + C_4 (S_{12} S_{23} + S_{13} S_{11}^* + S_{13} S_{33}^*) \right]
\end{aligned} \right\}
\end{aligned} \tag{31}$$

$$\begin{aligned}
& \frac{\partial \varepsilon_s \rho_s S_{23}}{\partial t} + \nabla \cdot (\varepsilon_s \rho_s \mathbf{v}_s S_{23}) \\
& + \varepsilon_s \rho_s (S_{21} W_{13} + S_{22} W_{23} - S_{13} W_{21} - S_{33} W_{23}) = \\
& \frac{\varepsilon_s \rho_s}{tr S} \left\{ \begin{aligned}
& 2 C_2 S_{11} S_{23} D_{11} \\
& + 2 C_2 S_{22} S_{23} D_{22} \\
& + 2 C_2 S_{33} S_{23} D_{33} \\
& + 2 C_2 S_{12} S_{23} D_{12} \\
& + 2 C_2 S_{13} S_{23} D_{13} \\
& + (2 C_2 S_{23} S_{23} + C_1 tr^2 S) D_{23} \\
& + f_c \|D\| \left[\begin{aligned}
& C_3 (S_{12} S_{13} + S_{22} S_{23} + S_{23} S_{33}) \\
& + C_4 (S_{12} S_{13} + S_{23} S_{22}^* + S_{23} S_{33}^*)
\end{aligned} \right]
\end{aligned} \right\}
\end{aligned} \tag{32}$$

Wu and Bauer equation

Status: Numerical Method

- Adopt ideas from Visco-elastic flow models
- FV methods are better than FE methods:
- memory usage, computational speed and stability (Huang et al., 1996, Wapperom and Webster 1998, Oliveira et al. 1998)
- At geometric singularities stresses are unbounded, but the force is finite

Status: Numerical Method

- Staggered mesh removes stress singularity and gives accurate results (Yoo and Na 1991; Sasmal 1995)
- Store components of stress at cell centers
- Derived wall boundary conditions: stress interpolation scheme indispensable for stability

Status: Numerical Method

- Derived discretization formulas
- Started coding for a two-dimensional problem. Mfix coding to begin soon
- Test problems
- startup Couette flow (analytical solution)
- L-valve
- chute flow

References

1. Huang, X., N. Phan-Thien, R.I Tanner, *J. Non-Newtonian Fluid Mech.*, **64**, 71-92 (1996).
2. Kolymbas, D., I.Herle, and P.A. Von Wolffersdorff, *Int. J. Numer Anal. Methods Geomech.*, **19**, 415-436 (1995).
3. Oliveira, P.J., F.T. Pinho, and G.A. Pinto, *J. Non-Newtonian Fluid Mech.*, **79**, 1-43 (1998).
4. Sasmal, G.P., *J. Non-Newtonian Fluid Mech*, **56**, 15-47 (1995).
5. Tejchman, J. and W. Wu, *Computers and Geomechanics*, **18**,71-84 (1996).
6. Wapperom, P., and M.F. Webster, *J. Non-Newtonian Fluid Mech.*, **79**, 405-431 (1998).
7. Wu, W., and E. Bauer, *Int. J. Numer Anal. Methods Geomech.*, **18**, 833-862 (1994).
8. Yoo, J.Y. and Y. Na, *J. Non-Newtonian Fluid Mech.*, **39**, 89-106 (1991).
9. Zhang, D.Z. and R.M. Rauenzahn, "A viscoelastic model for dense granular flows," *J. Rheol.*, **41**(6), 1997.

Application to 1D and 2D granular flows (no gas)

S. Benyahia

The reduction of this model to 2D flows is straightforward by assuming S_{33} , S_{13} and S_{23} equal to zero in equation 27-32. So we end up with the following three equations for the two normal components and one shear component of the stress tensor:

$$\frac{\partial \varepsilon_s \rho_s S_{11}}{\partial t} + \nabla \cdot (\varepsilon_s \rho_s v_s S_{11}) + \varepsilon_s \rho_s (S_{12} W_{21} - S_{21} W_{12}) = \frac{\varepsilon_s \rho_s}{tr S} \times \left\{ (C_2 S_{11} S_{11} + C_1 tr^2 S) D_{11} + C_2 S_{11} S_{22} D_{22} + 2 C_2 S_{11} S_{12} D_{12} + f_c \|D\| [C_3 (S_{11}^2 + S_{12}^2) + C_4 (S_{11}^{*2} + S_{12}^{*2})] \right\} \quad (33)$$

$$\frac{\partial \varepsilon_s \rho_s S_{22}}{\partial t} + \nabla \cdot (\varepsilon_s \rho_s v_s S_{22}) + \varepsilon_s \rho_s (S_{21} W_{12} - S_{12} W_{21}) = \frac{\varepsilon_s \rho_s}{tr S} \times \left\{ C_2 S_{11} S_{22} D_{11} + (C_2 S_{22} S_{22} + C_1 tr^2 S) D_{22} + 2 C_2 S_{12} S_{22} D_{12} + f_c \|D\| [C_3 (S_{12}^2 + S_{22}^2) + C_4 (S_{22}^{*2} + S_{12}^{*2})] \right\} \quad (34)$$

$$\frac{\partial \varepsilon_s \rho_s S_{12}}{\partial t} + \nabla \cdot (\varepsilon_s \rho_s v_s S_{12}) + \varepsilon_s \rho_s (S_{11} W_{12} - S_{22} W_{12}) = \frac{\varepsilon_s \rho_s}{tr S} \times \left\{ 2 C_2 S_{11} S_{12} D_{11} + 2 C_2 S_{22} S_{12} D_{22} + (2 C_2 S_{12} S_{12} + tr^2 S) D_{12} + f_c \|D\| [C_3 (S_{11} S_{12} + S_{12} S_{22}) + C_4 (S_{11}^* S_{12} + S_{12} S_{22}^*)] \right\} \quad (35)$$

For a 2D case, $S_{11}^* = \frac{1}{2}(S_{11} - S_{22})$ and $S_{22}^* = \frac{1}{2}(S_{22} - S_{11})$ so that $tr(S^*) = 0$.

For a 1D case solving for only one component of the normal stress, it's easy to just set $C_4 = 0$. Also it is clear that equation 35 cannot be solved for a traceless stress tensor, so that it is not possible to simulate a simple shear flow without a normal stress using this theory.

The components of the stress need not be positive. In fact we know by definition that the sum of all normal stresses must be negative because of the definition of pressure: $P_s = -\sum S_{ii}$. The shear stress S_{12} can, obviously, have either sign. Details of the implementation of the source terms in equations 33-35 is explained in a commented section at the beginning of scalar_prop.f.

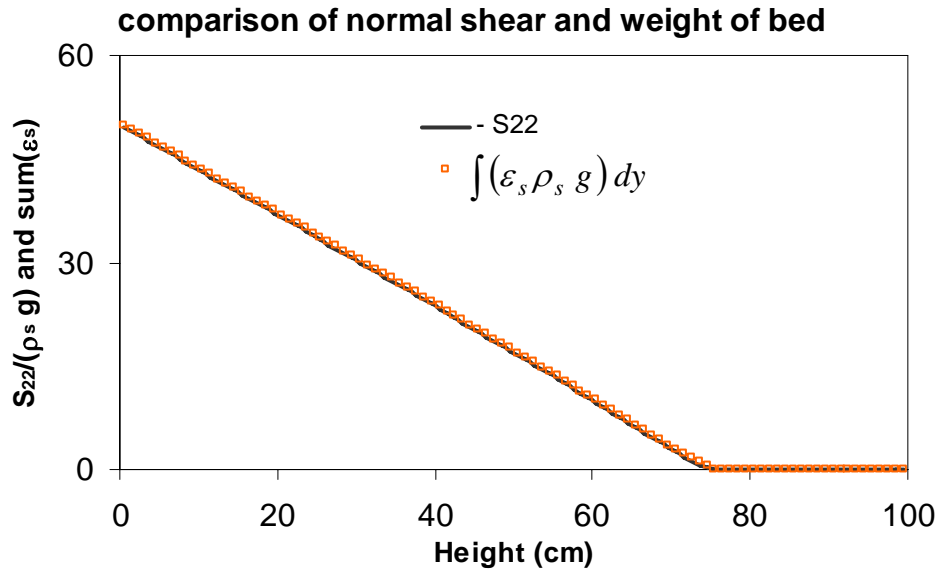
The effects of the stresses on the granular flow are implemented in the component i of the momentum equations as (Einstein summation notation is used for the repetitive j index):

$$\left[\frac{\partial}{\partial t} (\varepsilon_s \rho_s U_{si}) + \frac{\partial}{\partial x_j} (\varepsilon_s \rho_s U_{sj} U_{si}) \right] = \frac{\partial P^*}{\partial x_i} + \frac{\partial S_{ij}}{\partial x_j} + \varepsilon_s \rho_s g_i \quad (36)$$

In equation 36, the term $\frac{\partial S_{ij}}{\partial x_j} = \frac{\partial S_{i1}}{\partial x_1} + \frac{\partial S_{i2}}{\partial x_2}$, so that a normal and shear component of the stress

is added to both momentum equations. Also note that in equation 36 both the stress from hypoplastic theory and that from P^* are added to the momentum equation. However, P^* is only added for the cases in MFIx CVS identified as “withPstar”; otherwise, the call to compute P^* is commented in iterate.f subroutine, and thus P^* will have a value of zero.

The only case that gives reasonable results is the 1D settling case where at steady-state this balance is achieved: $-\frac{\partial S_{22}}{\partial y} = \varepsilon_s \rho_s g$ as shown in the following figure:



Other 2D cases show one major limitation of this theory as it is not able to prevent excessive packing of solids, so that these cases fail as void fraction approaches zero. So it was natural to add the solids pressure P^* that has been used in the conventional MFIX code to prevent this excessive packing. With P^* in the hypoplastic model, the results show a negligible effect of this new model as similar results are obtained without hypoplasticity.